Proceedings of the Intelligent Vehicles '92 Conference, Detroit, MI, June 29 - July 1, 1992.

Obstacle Detection for a Vehicle Using Optical Flow

Gin-Shu Young[1,2], Tsai-Hong Hong[1,3], Martin Herman[1], and Jackson C. S. Yang[2]

[1]National Institute of Standards and Technology (NIST), Bldg 220, Rm B124, Gaithersburg, MD 20899

[2]Robotics Laboratory, Department of Mechanical Engineering, University of Maryland, College Park, MD 20742

[3]Department of Computer Science and Information Systems, American University, Washington, D.C. 20016

Abstract

A novel approach to obstacle detection using optical flow without recovering range information has been developed. This method can be used for ground vehicles to navigate through man-made roadways or natural outdoor terrain or for air vehicles to land on known or unknown terrain. A linear relationship, plotted as a line and called a reference flow line, has been found. This reference flow line can be used to detect discrete obstacles above or below the reference terrain. Slopes of surface regions are also computed. The approach is simple, fast, and robust because (1) the only required information is one component of the optical flow, (2) each image line can be processed in parallel, and (3) the error sources involved are reduced to a minimum. An initial experiment using noisy synthetic data is also included to demonstrate the applicability and robustness of the method.

1 Introduction

Obstacle avoidance is one of the basic requirements in visual navigation. For autonomous vehicle operation in unstructured environments, obstacles must be detected before any obstacle avoidance activity can be taken. Obstacles are defined as any region in space where a vehicle should not or cannot traverse, such as steep terrain, protrusions (objects lying on top of the terrain), or depressions (potholes, ruts, gullies in the terrain). The goal of this paper is to develop a simple, fast, and robust method for obstacle detection by ground vehicles or during air vehicle landing. This would allow the ground vehicle to navigate through man-made roadways or natural outdoor terrain. This method would also allow the aircraft to land on known or unknown terrain.

Most existing methods (e.g. [2] [3] [4] [5] [7] [9] [16] [18]) perform obstacle detection based on *range information* obtained either from active sensors or passive sensors. Here, range is defined as the distance between the sensor and the object in the world. However, we have found that the geometry or shape of the object is sometimes more important than range for obstacle detection. In fact, we show it is possible to detect obstacles without direct range information.

One of the potential obstacle detection methods that does not utilize range information involves optical flow. Optical flow is the two dimensional motion observed in a camera's image. The optical flow results from the relative motion between the camera and the objects in the environment and represents the apparent motion of object points through a sequence of images. For example, figure 1 shows an optical flow field resulting from the translational motion of a camera mounted on a vehicle traveling on a planar road surface. The terrain that is close to the camera will appear to flow faster than the terrain that is distant. Optical flow, used by many biological creatures for navigation [1], is a very powerful method for obstacle detection. Herman and Hong [8] also described how optical flow can be used to perform real-time navigation, during both teleoperated low data rate driving and autonomous driving. One of the main advantages of using optical flow is that the ratio of distance to speed (e.g., time-to-collision) can easily be obtained and used for obstacle avoidance [10] [13]. Another advantage of using optical flow is that passive sensors, rather than active sensors such as laser scanners, are used. This eliminates radiation, reduces cost, and increases flexibility for many applications.

In this paper, a new method of obstacle detection using optical flow without recovering range information is developed. Discrete obstacles, as well as slopes of surface regions, are computed. In the following sections, previous work will be summarized first, then our method will be described. Following that, the equations derived for the method will be discussed and the results of our work will be presented. Finally, the features and advantages of the method will be summarized.

2 Previous Work

A number of obstacle detection methods have been developed in the past (e.g. [2] [3] [4] [5] [6] [7] [9] [11] [12] [14] [15] [16] [17] [18]). Range information is often employed to solve the problem of obstacle detection. This information may be obtained from active sensors (such as laser scanners, radars, and ultrasonics), stereo, optical flow, etc. *A priori* knowledge is also employed by most existing methods. Such knowledge may include road models (or maps), coordinate transformations, sensor motion, model optical flow fields, etc. Errors in *a priori* knowledge result in errors in the output. Even with perfect knowledge of road models or model optical flow fields, errors in the estimated data such as vehicle position or observed optical flow still result in errors in the output.

The following are some typical examples in which optical flow is used for obstacle detection. Nelson [11] detected discrete obstacles in free space using flow field divergence. Bhanu et al [2] presented an inertial sensor integrated optical flow technique for motion analysis. In their method, range information is extracted from optical flow for obstacle detection. Hoff and Sklair [9] detected landing hazards for a descending spacecraft. They developed an algorithm using range information retrieved from optical flow with known camera motion. Enkelmann [6] detected obstacles by evaluating the difference between calculated optical flow and estimated model flow. The estimated model requires knowledge about the focus of expansion (FOE), the transformation matrix between the camera and vehicle coordinate systems, and the camera motion. In addition, this method works only with a camera translating on a planar surface. Sridhar *et al* [16] at NASA Ames Research Center investigated the methodology for obstacle detection for rotorcraft low altitude flight. The obstacle detection problem is posed as the problem of finding range to all objects in the field of view. Range information is obtained by the use of optical flow. In addition to optical flow technology, stereo and integrated vision/active range sensors for obstacle detection are also under development in their research.

3 Method

As shown in the previous section, most existing technology for obstacle detection employs range information extracted from optical flow, stereo, or active range sensors. In addition, most obstacle detection technologies only deal with discrete obstacles (e.g., [5] [6] [11] [14] [15] [17]), while slope, a useful feature for determining traversability, is not calculated. In this paper, a new method of obstacle detection using optical flow without recovering range information is developed. The technique includes detection of discrete obstacles and calculation of terrain slope. This method can be used for ground vehicles navigating in man-made roadways or natural outdoor terrain or for air vehicles landing in known or unknown terrain.

For translational motion, if a line in space is projected into the image, then the component of optical flow perpendicular to this image line, as a function of position along the line, will result in a linear relationship. In figure 2a, if the line $\overline{AB}$ in space is projected into image line $\overline{ab}$, the component $\dot{y}$ of optical flow (extracted in a direction perpendicular to this image line) vs. image position x is a line (figure 2b). In figure 2a, the y coordinate of image line $\overline{ab}$ is y^* and the coordinates of the image points a and b are (x_o, y^*) and (x_n, y^*), respectively. The coordinates of the two points F_A and F_B in figure 2b are $(x_o, \dot{y}_o)$ and $(x_n, \dot{y}_n)$, respectively. The line $\overline{F_A F_B}$ in a plot of $\dot{y}$ vs. x is called a *reference flow line.* A proof of this property is found in section 4. The reference flow line will have enough information to indicate
(1) discontinuities in the flow field along the line and
(2) protrusions or depressions of 3-D objects relative to the line.

To apply the above properties to obstacle detection, three steps are involved.
Setp 1: Estimation of the reference flow line.
This line can be obtained from the observed optical flow corresponding to regions on the ground surface near the vehicle. In principle, only two points are required to estimate the reference flow line.
Step 2: Computation of the difference.
The difference between the reference flow line and the observed flow corresponding to objects projected into the image line is computed. Note that the "objects" here can be discrete obstacles or smooth or uneven terrain in the visible environment.
Step 3: Identification of terrain characteristics.
The computed difference in step 2 is used to identify the terrain characteristics. If the difference is positive, the observed point is considered to be a protrusion relative to the reference line (see figure 3). If the difference is negative, the observed point is regarded as a depression relative to the reference line.

Slopes of surface regions can also be computed. The formulas for calculating slope are derived in section 4. Many lines can be chosen in the image, to cover the full terrain ahead of the vehicle, and they can all be processed in parallel. An extension of this approach to general motion (translation and rotation) has also been developed [19].

The method has several features:

(1) Simple - Only one component of the optical flow is needed. In principle, normal flow, the component of the optical flow along the local gradient direction, can be used. The only assumption made is that the motion is a pure translation. Information such as a road or terrain model, specific knowledge of vehicle (or camera) motion, or knowledge of the coordinate transformation between the camera and the ground is not required. The feature used to detect discrete obstacles is simple - a straight line.
(2) Fast - The method is simple; therefore computation is fast. Each image line can be processed in parallel.
(3) Robust - Since the only required information is one component of the optical flow, the error sources involved are reduced to a minimum. The reference flow line is estimated from the observed data so that the reference and observed flows are from the same error source. This avoids multiple error sources, such as one error source from observed data and another from model data.

4 Derivation

In this section, it is proved that for an image line arising from a line in space, the relationship between one component of the optical flow and the image position is linear when the motion of the objects relative to the camera is translational. Following that the equations for calculation of terrain slope are introduced.

A reference flow line

Consider the line $\overline{AB}$ in space which is projected into the image line $\overline{ab}$. In figure 4, a coordinate frame c attached to the camera is chosen as follows:
(1) Let the camera focal point be the origin O_c.
(2) Let the optical axis be the Z_c axis.
(3) Choose X_c to be parallel to the image line $\overline{ab}$.
(4) Choose Y_c by the right hand rule.
A coordinate frame b is then affixed to the line $\overline{AB}$ as follows:
(1) Let the origin O_b be the point lying on the extended line $\overline{AB}$ with the shortest distance from the point O_c.
(2) Let the Z_b axis be along the line $\overline{AB}$.
(3) Choose X_b and Y_b by the right hand rule.
A point P in the scene can be transformed from frame b to frame c as follows:

$$\begin{Bmatrix} X_c \\ Y_c \\ Z_c \\ 1 \end{Bmatrix} = H_b^c * \begin{Bmatrix} X_b \\ Y_b \\ Z_b \\ 1 \end{Bmatrix} \tag{1}$$

where (X_c, Y_c, Z_c) and (X_b, Y_b, Z_b) are the coordinates of point P in frames c and b, respectively, and

$$H_b^c \equiv \begin{bmatrix} h_{11} & h_{12} & h_{13} & h_{14} \\ h_{21} & h_{22} & h_{23} & h_{24} \\ h_{31} & h_{32} & h_{33} & h_{34} \\ 0 & 0 & 0 & 1 \end{bmatrix} \tag{2}$$

represents a 4x4 transform matrix from frame b to frame c. Note that, for each instance of time, H_b^c is constant for all points in the scene. From the pinhole camera model, if we let the focal length be unity, the image position x is

$$x = \frac{X_c}{Z_c} \tag{3}$$

The equations for optical flow due to translational motion are as follows:

$$\dot{x} = \frac{1}{Z_c}(-T_X + xT_Z) \tag{4}$$

$$\dot{y} = \frac{1}{Z_c}(-T_Y + yT_Z) \tag{5}$$

where $(\dot{x}, \dot{y})$ are the components of optical flow, Z_c is the depth of the object relative to the camera, (x,y) are the components of the image position, and (T_X, T_Y, T_Z) is the translational motion of the object relative to the camera. Note that, for each instance of time, (T_X, T_Y, T_Z) are constants for all points lying on a rigid object. As defined earlier, line $\overline{AB}$ coincides with the Z_b axis, therefore any points lying on line $\overline{AB}$ always have

$$X_b = Y_b = 0 \tag{6}$$

With equations (1)(2)(3) and (6), the following linear relationship can be obtained from equation (5) for all image points lying on line $\overline{ab}$ that arise from points in the scene lying on line $\overline{AB}$:

$$\dot{y} = a_1 + a_2 x \tag{7}$$

where

$$\begin{aligned} a_1 &= \frac{h_{13}}{a_3} \\ a_2 &= \frac{-h_{33}}{a_3} \\ a_3 &= \frac{(h_{34}h_{13} - h_{14}h_{33})}{(-T_Y + yT_Z)} \end{aligned} \tag{8}$$

Equation (7) represents a reference flow line corresponding to one reference line in space. For each time, the values a_1, a_2, and a_3 are constants for all points on the reference line. Note that the reference flow line can be estimated from two points in principle (say, $(x_1, \dot{y}_1)$ and $(x_2, \dot{y}_2)$). This means that specific knowledge of the

transformation matrix and camera motion is not required.

Calculation of terrain slope

The terrain slope can be obtained from the optical flow without recovering range information. In figure 5a, the slope $\tan\alpha$ denotes the observed terrain $\overline{Q_1Q_2}$ relative to the reference line $\overline{P_1P_2}$. In figure 5b, the slopes $\tan\theta_1$ and $\tan\theta_2$ denote the reference line $\overline{P_1P_2}$ and the terrain $\overline{Q_1Q_2}$ relative to the line $\overline{O_cE}$. Here E is an image point with the coordinate (0,y). The components in the camera frame of the vectors $\overline{P_1P_2}$ and $\overline{O_cE}$ are ($x_{p2}Z_{p2}$-$x_{p1}Z_{p1}$, y(Z_{p2}-Z_{p1}), Z_{p2}-Z_{p1}) and (0, y, 1), respectively. With the components of the two vectors, the slope $\tan\theta_1$ for the line $\overline{P_1P_2}$ relative to $\overline{O_cE}$ can be found as

$$\tan\theta_1 = \frac{(x_{p2}K_p - x_{p1})}{(\sqrt{y^2+1}(K_p-1))} \tag{9}$$

where

$$K_p = \frac{Z_{p2}}{Z_{p1}} = \frac{\dot{y}_{p1}}{\dot{y}_{p2}} \tag{10}$$

and $\dot{y}_{p_1}$, $\dot{y}_{p_2}$ denote the y components of the optical flow at image positions x_{p_1} and x_{p_2}, respectively.
Similarily, the slope $\tan\theta_2$ for the line $\overline{Q_1Q_2}$ relative to $\overline{O_cE}$ can be found as

$$\tan\theta_2 = \frac{(x_{q2}K_q - x_{q1})}{(\sqrt{y^2+1}(K_q-1))} \tag{11}$$

where

$$K_q = \frac{Z_{q2}}{Z_{q1}} = \frac{\dot{y}_{q1}}{\dot{y}_{q2}} \tag{12}$$

and $\dot{y}_{q_1}$, $\dot{y}_{q_2}$ denote the y components of the optical flow at image positions x_{q_1} and x_{q_2}, respectively.
Finally, the terrain slope $\tan\alpha$ can be obtained as

$$\tan\alpha = \tan\theta_2 - \tan\theta_1 \tag{13}$$

5 Experiments and results

Two initial experiments using noisy synthetic data have been performed. The camera is mounted on the top of the vehicle 2 m above the ground (see figures 6 and 7). The first experiment involved detecting a bump a distance of 5 m from the head of the vehicle and a height of 0.3 m above the smooth terrain (see figure 6). The second experiment involved detecting a pothole with a depth of 0.6 m in the terrain as well as a ramp (see figure 7). The pothole was 6 m away from the vehicle and the beginning of the ramp was 12 m from the vehicle. The ramp was tested with various slope angles (9^o, 18^o, and 27^o).

In the first experiment, three kinds of noise were added to the optical flow field: 0% , 5%, and 10%. The results are presented in figures 8a, 8b, and 8c. The region above the horizontal line results from a protrusion above the terrain. The gap in the graphs at the end of the protrusion is due to occlusion. In the second experiment, for each slope angle (9^o, 18^o, and 27^o), there were two kinds of noise (0% and 10%) added to the optical flow field. The results are shown in figures 9a through 9f. The region below the horizontal line results from a depression in the terrain. The gap in the graphs at the beginning of the depression is due to occlusion. The region with a smoothly increasing value relative to the horizontal line denotes a ramp. The data points collected from the region were fit by a line. The slope of the line represented the slope of the ramp. The actual and calculated slopes of the ramp are presented in table 1 (the case without noise) and table 2 (the case with 10 % noise). The performance of this method depends on the quality of the input data. For example, this method may not work if the uncertainty in the range due to the optical flow value is larger than the size of the bump or pothole.

6 Conclusions

In this paper, a novel method of obstacle detection has been developed using optical flow without recovering range information. The method allows both detection of discrete obstacles and calculation of terrain slope. This method can be used for ground vehicles navigating in man-made roadways or natural outdoor terrain or for air vehicles landing in known or unknown terrain. The method has several advantages:
(1) Simple - Only one component of the optical flow is required. Knowledge about the road or terrain model, vehicle (or camera) velocity, or coordinate transformations is not needed (other than the assumption of translational motion).
(2) Fast - The amount of computation is small and each image line can be processed in parallel.
(3) Robust - Few error sources are involved.
The initial experiments included in the paper suggest that the approach using the reference flow line is effective and robust.

7 Acknowledgements

The authors would like to thank Jim Albus and David Coombs for important comments on this paper.

References

[1] J. S. Albus, T. H. Hong, "Motion, Depth, and Image Flow," *Proc. IEEE Int'l Conf. on Robotics and Automation*, 1990.

[2] B. Bhanu, B. Roberts, and J. Ming, "Inertial Navigation Sensor Intergated Motion Analysis for Obstacle Detection" *Proc. IEEE Int'l Conf. on Robotics and Automation*, 1990.

[3] M. J. Daily, J. G. Harris, and K. Reiser, "Detecting Obstacles in Range Imagery," *Proc. Image Understanding Workshop*, 1987.

[4] M. J. Daily, J. G. Harris, and K. Reiser, "An Operational Perception System for Cross-country Navigation," *Proc. Image Understanding Workshop*, 1988.

[5] R. T. Dunlay and D. G. Morgenthaler, "Obstacle avoidance on roadways using range data," *SPIE Mobile Robots*, Vol. 727, 1986.

[6] W. Enkelmann, "Obstacle Detection by Evaluation of Optical Flow Fields," *First Europen Conf. on Computer Vision*, 1990.

[7] M. Hebert and T. Kanade, "3D Vision for Outdoor Navigation by an Autonomous Vehicle," *Proc. Image Understanding Workshop*, 1988.

[8] M. Herman and T. H. Hong, "Visual Navigation using Optical Flow," *Proc. NATO Defense Research Group Seminar on Robotics in the Battlefield*, Paris, France, March 1991 .

[9] W. Hoff and C. Sklair, "Planetary Terminal Descent Hazard Avoidance Using Optical Flow ," *Proc. IEEE Int'l Conf. on Robotics and Automation*, 1990.

[10] D. N. Lee, "A theory of visual control of braking based on information about time-to-collision," *Perception*, Vol. 5, pp437-459, 1976.

[11] R. C. Nelson and J. Aloimonos, "Obstacle Avoidance using Flow Field Divergence," *IEEE Transactions on PAMI*, Vol. 11, No. 10, Oct. 1989.

[12] D. N. Oskard, T. H. Hong, and C. A. Shaffer, "Real-Time Algorithms and Data Structures for Underwater Mapping," *IEEE Trans. on Systems, Man, and Cybernetics*, Vol.20, No. 6, 1990.

[13] D. Raviv, "A Quantitative Approach to Looming," *NIST IR*, in preparation.

[14] S. Singh and P. Keller, "Obstacle Detection for High Speed Autonomous Navigation," *Proc. IEEE Int'l Conf. on Robotics and Automation*, 1991.

[15] U. Solder and V. Graefe, "Object Detection in Real Time," *SPIE Vol. 1388 Mobile Robots V*, 1990.

[16] B. Sridhar, R. Suorsa and P. Smith, "Vision Based Techniques for Rotorcraft Low Altitude Flight," *SPIE* , Vol. 1571, 1991.

[17] K. Storjohann, Th. Zielke, H. A. Mallot and W. Von Seelen, "Visual Obstacle Detection for Automatically Guided Vehicles," *Proc. IEEE Int'l Conf. on Robotics and Automation*, 1990.

[18] P. A. Veatch and L. S. Davis, "Range Imagery Algorithms for the Detection of Obstacles by Autonomous Vehicles," *Center for Automation Research Technical Report*, CAR-TR-309, July 1987.

[19] G.-S. Young, T. H. Hong, M. Herman, and J. C. S. Yang, "Visual Invariants, Optical Flow, and Obstacle Detection," in preparation.

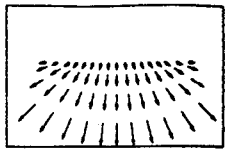

Fig. 1 Optical flow field due to translation

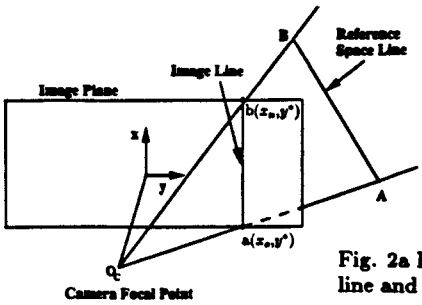

Fig. 2a Reference space line and image line

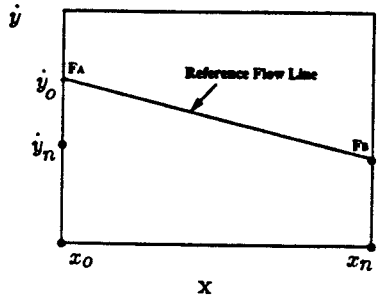

Fig. 2b Reference flow line

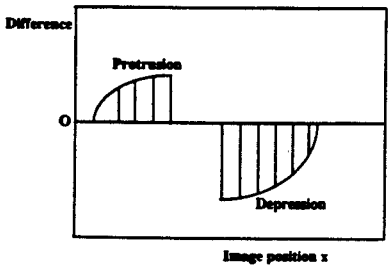

Fig. 3 Detection of discrete obstacles

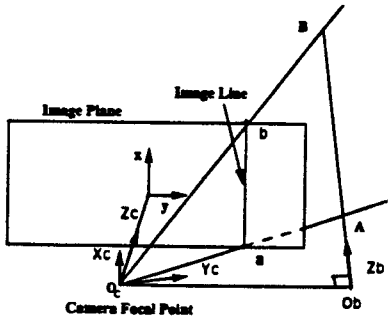

Fig. 4 Definition of two coordinate frames

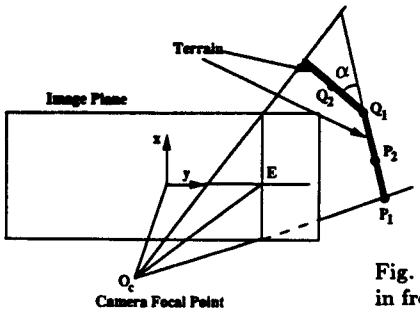

Fig. 5a Terrain slope in front view

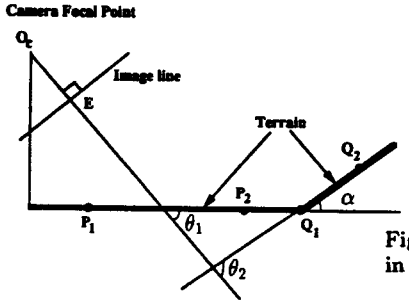

Fig. 5b Terrain slope in side view

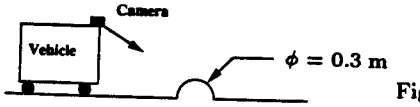

Fig. 6 Side view of terrain with a bump

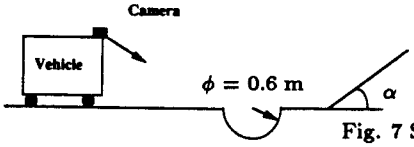

Fig. 7 Side view of terrain with a pothole and a ramp

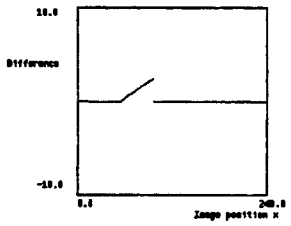

Fig. 8a Detection of a bump (0 % noise)

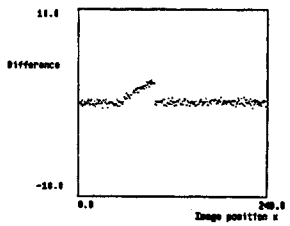

Fig. 8b Detection of a bump (5 % noise)

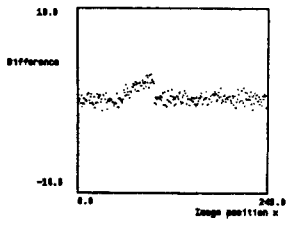

Fig. 8c Detection of a bump (10 % noise)

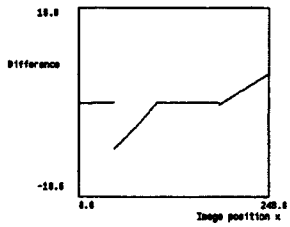

Fig. 9a Detection of a pothole and a 9° ramp (0 % noise)

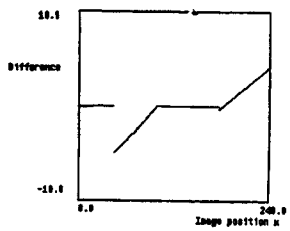

Fig. 9b Detection of a pothole and a 18° ramp (0 % noise)

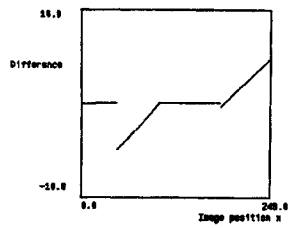

Fig. 9c Detection of a pothole and a 27° ramp (0 % noise)

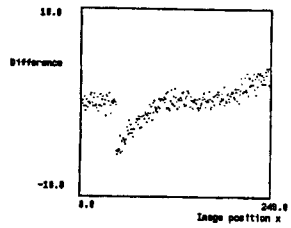

Fig. 9d Detection of a pothole and a 9° ramp (10 % noise)

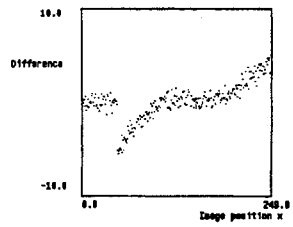

Fig. 9e Detection of a pothole and a 18° ramp (10 % noise)

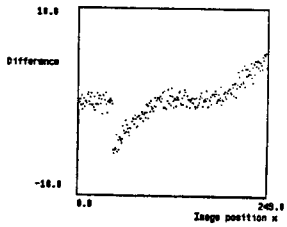

Fig. 9f Detection of a pothole and a 27° ramp (10 % noise)

Actual slope angles	9°	18°	27°
Estimated slope angles	9.29°	18.47°	27.52°

Table 1 Results of ramp detection with 0 % noise

Actual slope angles	9°	18°	27°
Estimated slope angles	8.27°	15.9°	23.13°

Table 2 Results of ramp detection with 10 % noise